Available online at www.sciencedirect.com
SCIENCE DIRECT®
Icarus 165 (2003) 371–378
ICARUS
www.elsevier.com/locate/icarus

Cratering rate on the jovian system: the contribution from Hilda asteroids

Adrián Brunini,* Romina P. Di Sisto, and Rosa B. Orellana

Facultad de Ciencias Astronómicas y Geofísicas and CONICET, Paseo del Bosque s/n (1900) La Plata, Argentina

Received 7 March 2003; revised 18 June 2003

Abstract

We study the dynamical evolution of the Hilda group of asteroids trough numerical methods, performing also a collisional pseudo-evolution of the present population, in order to calculate the rate of evaporation and its contribution to the cratering history of the Galilean satellites. If the present population of small asteroids in the Hilda's region follows the same size distribution observed at larger radii, we find that this family is the main contributor to the production of small craters (i.e., crater with diameters $d \sim 4$ km) on the Galilean system, overcoming the production by Jupiter Family Comets and by Trojan asteroids. The results of this investigation encourage further observational campaigns, in order to determine the size distribution function of small Hilda asteroids.

Keywords: Galilean satellites; Craters; Asteroids; Dynamical evolution; Resonances

1. Introduction

Impact cratering has been a natural and common process in the Solar System. The collision of bodies was a fundamental and frequent mechanism during planetary accretion. Although the impact rate has been decreasing as the Solar System was stabilizing, we have a considerable amount of evidence of an intense impact process in the past, for almost all the bodies of the Solar System. The impact process of the inner Solar System has been vastly studied, mainly, trough studies of lunar cratering.

To study the impact cratering history of bodies in the outer Solar System we have a natural and appropriate scenario, the four Galilean satellites: Io, Europa, Ganymede, and Callisto. Io has no known impact craters. Europa, is an icy world crossed by a network of dark fractures. The existence of few impact craters suggest that geologic processes are active today, and that it has a young surface. The largest Galilean satellite, the icy moon Ganymede, has a dark, heavily cratered terrain with more recent brighter grooved terrain. It also shows evidence of geologic activity, but its surface is very old, dating from the Late Heavy Bombardment or earlier. Also Callisto is very old. Its surface is completely saturated by craters. One feature unique to Callisto is the remnant structures of numerous impacts. The recent images obtained by the Galileo mission raise crucial questions about the nature of impactor populations in the jovian system.

Zahnle et al., 1998 (Z98), studied a number of populations that produced the craters on the Galilean satellites. They discussed in detail the Jupiter Family Comets (JFCs), using the numerical study of Levison and Duncan (1997). Other sources, like Long Period Comets, Trojan asteroids, and asteroids from the main belt were also considered. Z98 also analyzed the production of 10- and 20-km craters and estimated ages for Europa and Ganymede's surfaces.

Levison and Duncan (1997) performed a numerical simulation where the dynamical evolution of 2200 massless particles was followed for 1×10^9 yr, under the gravitational influence of the Sun and the four giant planets, from their origin in the Kuiper Belt. As a by product, they have calculated the impact rates of ecliptic comets on the planets. In particular they found for impacts on Jupiter one collision every 400 years; this number was found by directly counting the impacts during the simulation. Z98, used these data to characterize the orbits of JFCs encountering Jupiter, and using a Monte Carlo model, simulated the interaction of comets from this orbital distribution with Jupiter and its satellites, determining the impact velocities and relative impact probabilities with respect to Jupiter. They obtained that at least 90% of the cratering on the Galilean satellites is due to impacts by JFCs. Subsequently, Levison et al., 2000, reevaluated the impact rates on the planets from ecliptic

* Corresponding author.
E-mail address: abrunini@fcaglp.unlp.edu.ar (A. Brunini).

0019-1035/$ – see front matter
doi:10.1016/S0019-1035(03)00202-1

comets. They found that current impact rates on the giant planets are actually about four times smaller than in Levison and Duncan (1997). For Jupiter they calculated a value of 6.3×10^{-4} col. per yr or a collision every 1600 yr. So, the estimates done by Z98 for the Galilean satellites should be corrected by that factor. One uncertainty of those estimates is the relative importance of inactive comets. In this sense, another correction has to be done to the rates, taking into account a new estimate of the number of JFCs with $q < 2.5$ AU given by Bottke et al. (2002). Based on scaling the numbers of inactive comets, rather than active comets, they obtained that the number of kilometer-size comets in the JFC region is a factor of 3 lower than the estimates done by Levison et al. (2000). This factor directly affects the impact rates on the Galilean satellites, reducing by a factor of three the impacts by JFCs previously obtained. So the values in Z98 have to be reduced by a factor of 12.

For the Trojan asteroids, Z98 consider the fact that after Trojan asteroids escape from the resonance they follow an orbital evolution like that of JFCs. They stated that the ratio of trojans to all JFCs is 1/40, so depending on the Trojan mass distribution, they contribute at a 1–10% level to the craters on the Galilean satellites.

With respect to the main belt asteroids, Z98 used the analysis of Gladman et al. (1997) who studied the orbital evolution of asteroids escaped from unstable resonances. Scaling the impacts on the Galilean satellites to the NEA impact rate on the Earth, Z98 found that the contribution of asteroids from the main belt to the cratering rate on the Galilean system is negligible with respect to the one by JFCs. The well-known fact that the region of the main belt interior to the 3 : 1 mean motion resonance does not supply asteroids to the external region of the Solar System (Fernández et al., 2002) is probably the reason for this low value. However, the contribution to the cratering of the Galilean satellites by the external main belt was not analyzed in Z98, and so we have focused our attention to this zone.

The Hilda group of asteroids is placed in the 3 : 2 mean motion resonance with Jupiter. Taxonomically, they are mainly of P class and there are some D class, too. Their spectra may indicate mineralogies rich in low temperature materials, such as carbon compounds, complex organics, clays, water, and volatiles. The P and D taxonomic classes are probably transitional objects, between the rocky asteroids of the main belt and the volatile-rich comets in the Kuiper Belt and the Oort Cloud. The Hilda asteroids are an important population characterized by a great dynamical stability on its central zone where an asteroid can last for the age of the Solar System (Nesvorný and Ferraz-Mello, 1997; Ferraz-Mello et al., 1998). However, this thin zone is surrounded by a strongly unstable boundary, where the characteristic permanence times are very short. Therefore an asteroid entering in these zones is quickly ejected from the resonance.

In this paper we study the dynamical evolution of Hilda asteroids escaping from the resonance and performed a collisional pseudo-evolution, in order to calculate their contribution to the cratering history of the Galilean satellites.

The paper is organized as follows: In Section 2 we present the initial conditions and the relevant results of the numerical simulation of the dynamical evolution of a sample of a fictitious population of asteroids in the 3 : 2 mean motion resonance with Jupiter. In Section 3 we perform the scaling of impacts onto Jupiter vs. impacts onto the Galilean satellites. Section 4 is devoted to studying the population of real Hilda asteroids and the rate of evaporation of the population due to catastrophic collisions. In Section 5 we compute the cratering rate on the Galilean satellites and the last section is devoted to the conclusions.

2. Initial conditions and numerical simulation

We have performed a numerical integration of 500 mass less particles under the gravitational influence of the Sun and the planets from Mercury to Neptune, with the hybrid simplectic integrator EVORB (Fernández et al., 2002). The initial conditions of the objects in semi major axis, eccentricity and inclination were generated at random, but following the distributions of orbital parameters of the real Hilda asteroids, taken from the asteroid data base of the Lowell Observatory. The distributions in the space of orbital elements a, e, i are shown in Fig. 1. We are not interested here in the stability of asteroids inside the 3 : 2 resonance, nor in the rate of the dynamical "evaporation" of the resonance, but in the dynamical evolution the asteroids follow after escape from the resonance. At present, the main mechanism of evaporation of the resonance is collisional evolution. Gil Hutton and Brunini (2000) have shown that mutual collisions may

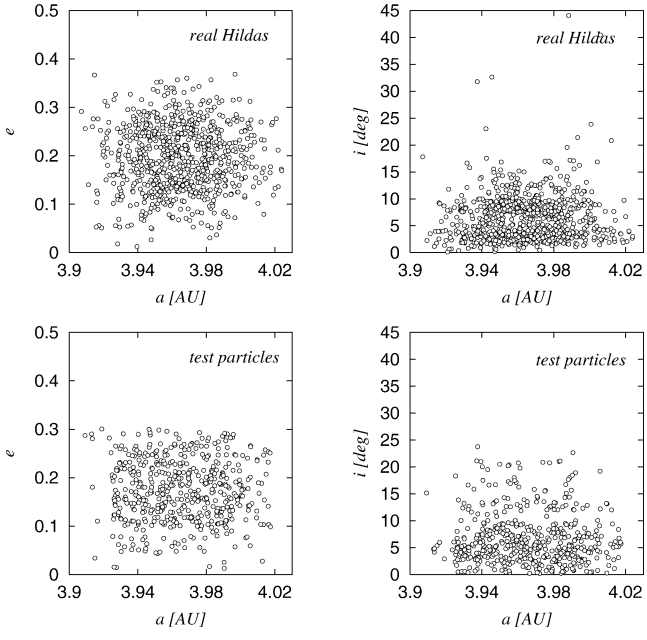

Fig. 1. Orbital elements of the real population of Hilda asteroids and distribution of the same elements of our fictitious test particles.

change the orbital elements of stable Hilda asteroids, moving them to unstable regions, where they can escape shortly after. In addition, a collision also changes the critical angle (Ferraz-Mello, personal communication). For this reason, the initial longitude of the perihelion, ascending node and mean anomaly were generated at random, so our test particles are not, in general, resonant objects, but representative of fragments recently moved from their original stable orbits. The sample was integrated for 1×10^9 yr.

After the total time span of the numerical integration, nearly 80% of the objects left the region of the Hilda asteroids. In the way we have generated the initial conditions, this number cannot be interpreted as representative of the rate of dynamical evaporation of the Hilda group, and in fact it will be not used in our further calculations. In Section 5 we will analyze the evaporation rate of the Hilda group in detail.

The information extracted form the simulation that will be used in our further calculations is the following

1. 8% of the objects leaving the resonance end up impacting Jupiter. By comparison, the fraction of Jupiter Trojans that, after leaving both the L4 and L5 swarms, end up colliding Jupiter, is only of about 2% (Fernández and Mallada, personal communication, 2002). It is also significant compared with the 2% of JFCs that hit Jupiter in the Levison and Duncan (1997) simulation.
2. The relative velocity of impact between escapees from the Hilda region and the Galilean satellites. Rather than using any approximation, it was possible to compute it directly from the simulation. We have recorded positions and velocities relative to Jupiter in about 3×10^4 close encounters at less than 2 Hill radii, at very small time steps. Therefore, it was possible to obtain the relative velocity of the objects with respect to Jupiter when they were at a distance from the planet comparable to the orbital semi major axes of the Galilean satellites. We have defined spherical shells centered at Jupiter, with a mean radius equal to the orbital semimajor axis of each Galilean satellite, and with a half width of about $\pm 5\%$ of each satellite physical radius. As the geometry of the encounters within 2 Hill's radii of Jupiter is near isotropic, the mean velocity of all the objects entering these shells are representative of the typical relative velocity when the objects intersect the orbit of each one of the Galilean satellites. The values so obtained are summarized in Table 1. Varying the 5% threshold from 1 to 10%, only affects the dispersion of the means, but the means themselves vary by less than 3%.

As our initial conditions have been not generated in a way self consistent with a collisional process, we have repeated our calculations dividing the sample of escaped particles in two subsamples: one with the particles escaped during the first 500 Myr, and a second subsample with the ones escaped during the last 500 Myr (i.e., those particles from more stable regions). We have not observed statistically significant differences.

Table 1
Satellite data and impact velocities

	Io	Europa	Ganymede	Callisto
a_s	5.9	9.4	15.0	26.4
r_s	1820	1570	2630	2400
v_s	17.3	13.7	10.9	8.2
v_0	24.3 ± 0.5	19.6 ± 0.4	15.7 ± 0.1	12.0 ± 0.1
$v_{\rm imp}$	29.6	23.7	19.1	14.5
$\dot{N}_{\rm sat}/\dot{N}_{\rm Jupiter}$	1.32×10^{-4}	6.32×10^{-5}	1.17×10^{-4}	5.93×10^{-5}

a_s: semi major axis of the satellite [jovian radii]. r_s: satellite geometrical radii [km]. v_s: satellite orbital velocity [km s^{-1}]. v_0: mean velocity of Hilda asteroids when they intersect the Galilean satellite orbit [km s^{-1}]. $v_{\rm imp}$: mean velocity of impact onto each Galilean satellite [km s^{-1}]. $\dot{N}_{\rm sat}/\dot{N}_{\rm Jupiter}$: rate of impacts onto each Galilean satellite/rate of impacts onto Jupiter.

The velocity of impact on the Galilean satellites was computed assuming that the geometry of the collisions is isotropic. In this situation, if the satellite orbital velocity is v_s, the most probable collision velocity may be computed as

$$v_{\rm imp} = \sqrt{v_s^2 + v_0^2}, \tag{1}$$

where v_0 is the mean velocity of Hilda asteroids, when they intersect the Galilean satellite orbit.

The values of the collision velocities, listed in Table 1, are very similar to the ones computed by Z98 for impacts of Jupiter family comets onto the Galilean satellites, and differ only in about 10%.

3. Impact rate on the Galilean satellites

It is possible now to obtain the probability of impact on each Galilean satellite, relative to probability of impact onto Jupiter. In principle, there are several ways to compute these values, and we follow the very easy procedure derived by Harris and Kaula (1975). The relative impact rate is given by

$$\frac{\dot{N}_{\rm sat}}{\dot{N}_{\rm planet}} = \left(\frac{r_s}{r_p}\right)^2 \left(\frac{1 + 7\theta r_p/r_s}{1 + 2\theta}\right), \tag{2}$$

where r_s and r_p are the satellite and planetary radii, respectively, and θ is a dimensionless parameter first introduced by Safronov (1969), whose expression is

$$\theta = \frac{G m_p}{r_p v_\infty^2}, \tag{3}$$

where m_p is the planetary mass, G the constant of gravitation, and v_∞ is the relative velocity of the objects when entering in the Hill's sphere of the planet. In our case, it was possible to compute this relative velocity, in a fashion very similar to the one used to compute v_0, being $v_\infty = 5.45$ km s^{-1}, which is very similar to the value for Jupiter

family comets obtained by Z98, of $v_\infty \sim 5$ km s^{-1}. Therefore, as the only different parameter entering in Eq. (1) for these two populations is the relative velocity, we would expect very similar results for the probability of impacts on Jupiter for Hildas and JFC. The values of $\dot{N}_{\rm sat}/\dot{N}_{\rm Jupiter}$ are shown in Table 1, where it is possible to observe that the relative differences with the values shown in Z98 (in their Table I) for JFC, and obtained by means of a more sophisticated Öpik formalism, are less than 6%.

4. Hilda population

As of October 31, 2002, 814 Hilda asteroids were cataloged in the asteroid data base of the Lowell Observatory (http://asteroid.lowell.edu). From this sample, a subsample of 35 asteroids have had their diameters estimated. Fig. 2 displays the relation between the diameter D, and the cataloged absolute magnitude H of this sub-sample. Also shown in Fig. 2 is a least square fit of the form

$$\log D(\text{km}) = sH + b, \tag{4}$$

where $s = -0.189 \pm 0.01$ and $b = 3.673 \pm 0.14$. Extrapolating this fit to the whole sample (i.e., assuming that the mean geometric albedo does not change with size), it is possible to estimate the diameters of the entire population. The cumulative number of objects with diameter greater than D_0, $N(> D_0)$, is shown in Fig. 3. Although the sample at very large sizes should not be included, since it has not been affected by collisional evolution, it is possible to perform a unique power law fit to the cumulative number of objects of the sample, up to $D \sim 12$ km, of the form

$$N(> D_0) \propto D_0^q, \tag{5}$$

revealing that the observed sample is complete up to this diameter, a result already reported by Davis et al. (2003). The best fit is obtained for $q = -2.11 \pm 0.008$, which agrees with an outcome of a collisional cascade. Roig et al. (2002) have performed a similar study, found $q = -2.17$. It is worth noting that q is not too sensible to the upper limit included in the sample.

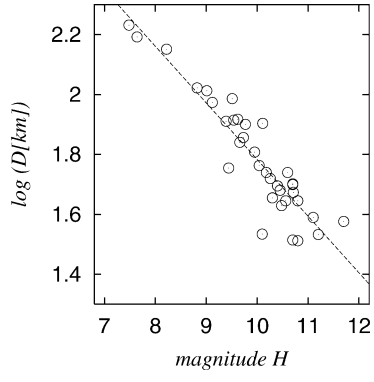

Fig. 2. Known Hilda asteroids with well determined diameters and the least square fit of the relation between the absolute magnitude H and the diameter in km.

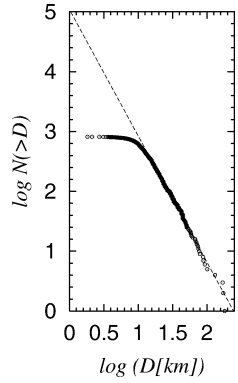

Fig. 3. Population of all known Hilda asteroids. The slope of the least square fit to the relation between $\log(N)$ and $\log(D)$ is $q = -2.11 \pm 0.008$.

Extrapolating to smaller diameters with this exponent, we obtain a total population of Hildas larger than $D_0 = 2$ km (i.e., radius $r = 1$ km) of about 25000 asteroids, which is about 8% of the estimated population at the L4 and L5 Trojan swarms, of about 3.2×10^5 objects (Jewitt et al., 2000). As it is the case for Trojan asteroids, there is no generalized consensus about the Hilda population at small diameters, and a smaller population than the number quoted above is possible (Davis et al., 2003). Therefore, more observations are needed in order to shed light on this question.

With all these information at hand, it is possible now to compute the diameter of a simple crater produced by objects from the Hilda region. We have used the same expressions recommended by Schmidt and Housen (1987). They propose to use the scaling relation

$$d_s = 1.4\left(\frac{m_a}{2\rho_s}\right)^{0.26}\left(\frac{\rho_a}{\rho_s}\right)^{0.073} g_s^{-0.22} v_{\rm imp}^{0.44}\ \text{cm}, \tag{6}$$

where m_a and ρ_a are the mass and density of the impactor that we have assumed to be 2.5 g cm^{-3}, ρ_s is the density of the target and g_s its surface gravity. It is worth noting that the crater diameter is rather insensitive to the bulk density adopted for the projectile. This expression is to be evaluated in cgs units. It is worth noting that the uncertainty in crater diameter for a given impactor is probably about 30%. We have also included an additional correction for complex craters, because larger craters are considerably shallower and wider than the simple crater described by Eq. (6). For crater diameters $d_s > d_c$ predicted by Eq. (6), the final crater diameter is computed by (McKinnon et al., 1991)

$$d = d_s^{1.13} d_c^{-0.13}, \tag{7}$$

where d_c is the transition between simple and complex crater structure. Following Chapman and Mc Kinnon (1986), we adopted a value of $d_c = 4$ km for craters on Ganymede. The numerical coefficient in Eq. (6) was computed considering the most probable incident angle of 45°.

Table 2
Population of Hildas capable of producing craters with $d > 10$ km

Satellite	m_a	D_a	$N(> D_a)$
Io	1.86E+14	0.522	4×10^5
Europa	3.68E+13	0.304	13×10^5
Ganymede	5.72E+13	0.352	10×10^5
Callisto	8.10E+13	0.396	8×10^5

Population of Hilda asteroids capable of producing craters with $d > 10$ km as computed from our cumulative size distribution function. m_a is the minimum mass [g] of a Hilda asteroid capable of producing a crater of $d = 10$ km on each one of the Galilean satellite. D_a is the corresponding asteroid diameter [km], assuming a bulk density of 2.5 g cm^{-1}. $N(> D_a)$ is the number of Hilda asteroids larger than this diameter.

Table 2 shows the estimated population of Hilda asteroids capable of producing craters of $d > 10$ km on each one of the Galilean satellite.

5. Rate of evaporation of the Hilda asteroid resonant group by collisions

Hilda asteroids from the stable zone may reach the unstable boundary of the resonance following some dynamical route. In general, these routes of diffusion are very slow, and the evaporation rate of the resonance is very slow too. However, the Hilda asteroids form a population subject to a strong collisional evolution. As for Trojans, exchange of impulse during collisions is the most efficient way to reach the unstable regions of the boundary of the resonance and escape from it. Therefore, to compute the rate of evaporation of the Hilda swarm, a collisional evolution model should be studied. As our interest is limited to compute the present rate of evaporation, we have performed only one step in the process of collisional evolution of the population, following the prescriptions of Davis et al. (2003) and Gil Hutton and Brunini (2000), i.e., a sort of a collisional "pseudo-evolution," where the population is considered in steady state. In a real collisional evolution, the population evolves, therefore we are considering that this evolution is at present slower than the relevant time scales involved in our problem.

To study the collisional evolution of the Hilda population we will look for catastrophic collisions, which as usual, are defined as the collisions where the largest piece resulting from them contains 50% or less of the initial target mass. The radius r_p of the smallest projectile capable of shattering a target with radius r_a is (Davis et al., 1989)

$$r_p = r_a \times \left(\frac{4S}{\rho_a v^2}\right)^{1/3}, \tag{8}$$

where ρ_a is the density of the asteroid, $v = 4.6$ km s^{-1} the collision velocity (Gil Hutton and Brunini, 2000) between Hildas, and S is the impact strength. For this last parameter, we used the energy scaling algorithm recommended by Davis et al. (1994)

$$S = S_0 + \frac{4\pi k G \rho_a^2 r_a^2}{15}, \tag{9}$$

where $S_0 = 3 \times 10^7$ erg cm^{-3}, G is the gravitational constant and k is a dimensionless parameter, that we have adopted, following Davis et al. (2003), equal to one.

Then the catastrophic collision probability per unit time, of an asteroid of radius r_a is

$$P(r_a) = P_i \int_{r_p}^{r_{\max}} (r_a + r)^2 n(r)\, dr, \tag{10}$$

where $r_{\max}$ is the largest object in the population, P_i is the intrinsic probability of collision and $n(r)$ is the differential size distribution of the population. For the case of the Hilda asteroids, we have obtained $n(r) \propto r^{-3.11}$. For the Hilda asteroids we adopted $P_i = 0.65 \times 10^{-18}$ km^{-2} yr^{-1} (Gil Hutton and Brunini, 2000). These set of values are different than those found by Dell'Oro et al. (2001), i.e., $P_i = 1.93 \times 10^{-18}$ km^{-2} yr^{-1} and $v = 3.14$ km s^{-1}. These differences probably arise from the different methods of computing them. Nevertheless, a computation with this set have not offered noticeable differences in our final results (within a 7%). It is probably due to the fact that a higher intrinsic probability of collision P_i is partially compensated by a lower typical collision relative velocity v. Per unit time, the number of asteroids of radius r_a receiving a catastrophic collision is given by

$$N_{\rm col}(r_a) = N(r_a) P(r_a), \tag{11}$$

where $N(r_a)$ is the number of objects with radius r_a.

The outcome of a catastrophic collision is a number of fragments, distributed in an incremental size distribution of the form

$$N(> m) \propto m^{-p} \tag{12}$$

(Greenberg et al., 1978; Zapalá et al., 1984; Fujiwara et al., 1989), where $N(> m)$ is the number of fragments having masses larger than m. The exponent p is a function of the mass of the largest fragment normalized to the mass of the original body m_a. Equations (8) to (12) allow us to compute the number of fragments larger than a given diameter produced in the Hilda region by unit time. However, only a fraction of the fragments can escape the gravitational attraction of the largest body and eventually, if the velocity is high enough, can also escape from the resonance. The cumulative velocity distribution of the fragments is modeled with the usual formulation (Gault et al., 1963)

$$f(> V) = (V/V_0)^{-9/4}, \tag{13}$$

$f(> V)$ is the fraction of objects moving faster than V, and V_0 is a lower cutoff for the fragment velocities, which is obtained from the energy partitioning coefficient defined as the fraction of the collisional kinetic energy which goes with the fragment motion, and is often taken to be between 1 and 10%. We have adopted the conservative value of 2%, although we have carried out experiments exploring all the range of possible values not obtaining too different results.

To compute the number of fragments escaping from the resonance, we adopted the same prescription as in Gil Hutton and Brunini (2000). If the fragment acquires a small impulse, its orbital velocity changes a small amount ΔV. In this situation we can write, by means of Gauss' equations

$$\Delta a = \frac{2}{n}\Delta V_T, \tag{14}$$

where ΔV_T is the component of ΔV in the direction of motion, a is the semimajor axis of the fragment and n is the mean motion. From Ferraz-Mello et al. (1998) we obtain $\Delta a \sim 0.05$ AU as the half width of the stable region, therefore, a fragment originally placed at the center of the resonance can reach its unstable boundaries if its velocity is incremented by an amount of $\Delta V_T > 0.094\ \mathrm{km\,s^{-1}}$. If the relative velocities of collisions between the projectile and the target are assumed equally partitioned between the three components, the ejection velocity needed to escape the resonance is $\Delta V > 0.163\ \mathrm{km\,s^{-1}}$. It should be compared with the ejection velocity obtained by the same procedure for the Trojan asteroids, which is of $0.65\ \mathrm{km\,s^{-1}}$, i.e., four times higher than for Hilda asteroids, revealing that the Trojan population is dynamically more stable against collisions.

Equations (8) to (14) are therefore the relations that allow us to compute the rate of production of fragments larger than a given diameter escaping from the resonance as a result of the collisional evolution.

Cratering collisions should also be considered, although the exchange of impulse during this kind of event is less effective to produce ejection from the resonance. It is worth noting also that in this case only one object (if any) can escape from the resonance at each collision, so the contribution from this regime to the cratering history of the Gallilean satellites should not be important.

6. Cratering rate

With all this information at hand it is possible to compute the rate of production of fragments escaping from the Hilda swarm, and capable of producing craters larger than a given diameter on each one of the Galilean satellites. We assume that after escaping from the resonance by collisional evolution, the asteroids will follow a dynamical evolution similar to the one obtained in our simulation (see Section 2). Therefore only 8% of the fragments escaped from the resonance will end up impacting Jupiter, and only a small fraction, which is given in Table 1, will impact a given Galilean satellite. As we have computed the rate of escape form the Hilda region in the preceding section, it is possible to compute the rate of impact on each one of the Galilean satellite. The rate of production of craters ($\dot{C}$), larger than a given diameter, may be now computed from the expressions given in Section 4.

The results of these calculations are shown in Table 3 in terms of the smallest target diameter r_a to which the size distribution function at larger diameters may be extrapolated, because this is the main uncertainty factor in our calculations.

Table 3
Cratering rate for craters with d > 10 km

$r > r_a$ [km]	$\dot{C}_I^{-1}$ [y]	$\dot{C}_E^{-1}$ [y]	$\dot{C}_G^{-1}$ [y]	$\dot{C}_C^{-1}$ [y]
0.4	2.1×10^7	1.5×10^7	1.1×10^7	2.6×10^7
0.6	6.9×10^7	4.9×10^7	3.6×10^7	8.9×10^7
0.8	1.6×10^8	1.2×10^8	8.4×10^7	2.1×10^8
1.0	3.2×10^8	2.3×10^8	1.6×10^8	4.1×10^8
1.5	1.1×10^9	7.7×10^8	5.5×10^8	1.4×10^9
(JFC)	2.6×10^7	1.5×10^7	1.0×10^7	2.6×10^7

$\dot{C}^{-1}$: Mean interval between impacts on the Galilean satellites in years, capable to produce craters with $d > 10$ km. r_a is the radius of the minimum target considered to be member of the Hilda population. The last row are the mean intervals between craters with $d > 10$ km computed by Z98 for JFC, and corrected by the factor of 12.

It is worth noting that we are considering that the Hilda population follows the same cumulative size distribution function up to very small diameters. Not only the diameters of the small targets but the much smaller diameters of the smallest projectile capable to shatter them. For example, the diameter of the smallest projectile capable of shattering an asteroid of $D = 400$ m is of about $D = 20$ m.

However, the current observational cumulative size distribution function of the Hildas shows a break of the slope in $D = 12$ km (see Fig. 2). The small width in semimajor axis of the resonance, and the low escape velocity from it, means that small fragments produced by collisions closer to the boundary of the resonance can easily escape. This could produce a depletion of the Hildas size distribution for low diameters and a permanent loss of small fragments, (Gil Hutton and Brunini, 2000). On the other hand, the collisional evolution produces small objects from greater ones, so this could balance the low diameter depletion.

However, a high collisional activity at present seems to be not compatible with a collisionally relaxed population. Therefore, following Davis et al. (2003) we assume that the change of slope observed at $D \sim 12$ km is due to an observational selection, and under this assumption (i.e., that the Hildas follow the same size distribution at smaller radii), the crater production from Hilda asteroids is comparable to the rate of production by Jupiter Family Comets. We give our results in terms of the smallest target considered in the collisional evolution model.

Europa has only 27 known craters with $d > 4$ km (Moore et al., 2001). Although Bierhaus et al. (2001) states that the vast majority of small craters are secondaries, probably all craters larger than 2 km are primary craters. So, $d > 4$ km seems to be a safe election for primary craters. In Table 4 we give the same information than in Table 3 but for craters with $d > 4$ km. It is possible to see that different considerations regarding the population of the Hilda group at smaller diameters may change substantially the determination of the age of Europa's surface features, although in any case it is very young.

Table 4
Cratering rate for craters with d > 4 km

$r > r_a$ [km]	$\dot{C}_I^{-1}$ [y]	$\dot{C}_E^{-1}$ [y]	$\dot{C}_G^{-1}$ [y]	$\dot{C}_C^{-1}$ [y]
0.2	2.5×10^5	2.3×10^5	1.6×10^5	4.1×10^5
0.4	2.0×10^6	1.8×10^6	1.3×10^6	3.3×10^6
0.6	6.7×10^6	6.2×10^6	4.4×10^6	1.1×10^7
0.8	1.6×10^7	1.5×10^7	1.0×10^7	2.6×10^7
1.0	3.1×10^7	2.9×10^7	2.0×10^7	5.1×10^7
2.0	2.5×10^8	2.3×10^8	1.6×10^8	4.1×10^8
3.0	8.3×10^8	7.7×10^8	5.5×10^8	1.4×10^9

$\dot{C}^{-1}$: Mean interval between impacts on the Galilean satellites, capable to produce craters with $d > 4$ km.

We want to mention that the last rows in Tables 3 and 4 should be taken with caution, because the time intervals are too long as to neglect the evolution of the Hilda population due to collisional evolution.

It is worth noting that two stable populations relatively isolated from the main asteroid belt (i.e., Trojan and Hilda asteroids), have such different contributions to the cratering rate of the Galilean satellites. The population of Trojans is probably 13 times the population of Hilda asteroids, however:

- The intrinsic collision probability for Hildas is 2 times higher than for Trojans (Gil Hutton and Brunini, 2000), so, although the Hilda region is 13 times less populated than both Trojan swarms, collisions are only $13/2 = 6.5$ times less frequent than among Trojans.
- Another factor of $1/2$ must be considered, because the Trojans are occupying two almost independent groups (i.e., the L4 and L5 swarms).
- The fact that the escape velocity of Trojans is four times the one for Hildas, makes it more difficult a fragment to escape from the resonance (the Trojans are more stable than the Hildas against evaporation due to collisional evolution).
- Numerical simulations of the dynamical evolution of the Trojan swarms (Fernández and Mallada, 2002, personal communication), have shown that only 2% of escaped Trojans impact Jupiter. This is a low value compared with the 8% for the Hildas.

All these factors together make the Hilda contribution to the cratering rate on the Galilean satellites to be 4–5 times more important than the one due to the Trojan asteroids.

A major difference between the cratering rates from Hilda asteroids and JFC is regarding the time-scales involved in the process. As it is shown in Fig. 4, nearly 75% of the objects that impact Jupiter do so in less than 5×10^4 yr after escape from the resonance. It represents a very short time as compared with the 40 Myr that typically spends a comet to travel from the Kuiper Belt to the Jupiter region (Levison and Duncan, 1997). We could speculate that after a catastrophic collision, many fragments escape from the Hilda region. A considerable number of them end-up colliding Jupiter ($\sim 8\%$) during the relatively short time interval of some 10^4 yr. If some signature of this kind of process is found on the surfaces of the Gallilean satellites, it would furnish important clues regarding the past history of the Hildas.

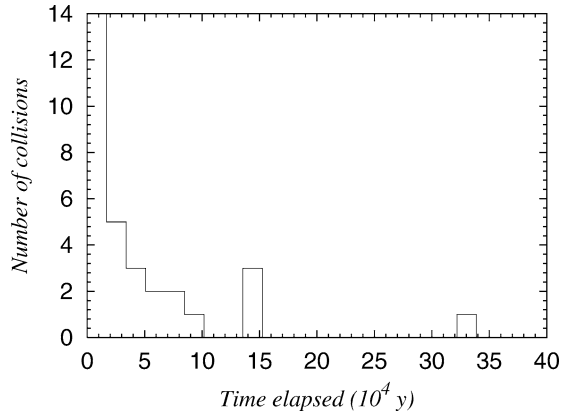

Fig. 4. Distribution of the time elapsed after escape from the 3 : 2 resonance, up to the collision with Jupiter, for 31 asteroids from the simulation, with this end-state.

7. Conclusions

We have found that the Hilda asteroid population could be the main source of small impact craters on Jupiter satellites, even overcoming the contribution from JFCs. From our numerical simulations of the dynamical evolution of fictitious Hilda asteroids, we have obtained that 8% of the particles that leave the resonance hit Jupiter. None of them hit the terrestrial planets. In contrast, Z98, based in the numerical simulation made by Gladman et al. (1997) about the dynamical evolution of objects in asteroid belt resonances interior to 3.5 AU, demonstrated that the main asteroid belt contributes a negligible fraction to the Galilean satellite cratering. One could say that the cratering history of the inner and outer Solar System is different, and the fact that a compact population such as the Hilda family could be the main source responsible for the production of small craters in the zone of Jupiter, makes us think that the catering histories of bodies of the outer Solar System have to be separately analyzed.

Acknowledgments

We acknowledge the support by the Instituto Astrofísico de La Plata of the CONICET. We also acknowledge the constructive criticisms of the two referees that helped us to improve the manuscript.

References

Bierhaus, E.B., Chapman, C.R., Merline, W.J., Brooks, S.M., Asphaug, E., 2001. Pwyll Secondaries and other small craters on Europa. Icarus 153, 264–276.

Bottke, W.F., Morbidelli, A., Jedicke, R., Petit, J., Levison, H., Michel, P., Metcalfe, T.S., 2002. Debiased orbital and size distribution of the near-Earth objects. Icarus 156, 399–433.

Chapman, C.R., Mc Kinnon, W.B., 1986. Cratering on planetary satellites. In: Burns, J.A., Matthews, M.S. (Eds.), Satellites. Univ. of Arizona Press, Tucson, pp. 507–553.

Davis, D.R., Weidenschilling, S.J., Farinella, P., Paolicchi, P., Binzel, R.P., 1989. Asteroid collisional history: effects on sizes and spins. In: Binzel, R.P., Gehrels, T., Matthews, M.S. (Eds.), Asteroids II. Univ. of Arizona Press, Tucson, pp. 805–826.

Davis, D.R., Durda, D.D., Marzari, F., Campo Bagatin, A., Gil Hutton, R., 2003. Collisional evolution of small-body populations. In: Bottke Jr., W.F., Cellino, A., Paolicchi, P., Binzel, R.P. (Eds.), Asteroids III. Univ. of Arizona Press, Tucson, pp. 545–558.

Davis, D.R., Ryan, E.V., Farinella, P., 1994. Asteroid collisional evolution: results from current scaling algorithms. Planet. Space Sci. 42, 599–610.

Dell'Oro, A., Marzari, F., Paolicchi, P., Vanzani, V., 2001. Updated collisional probabilities of minor body population. Astron. Astrophys. 366, 1053–1060.

Fernández, J.A., Gallardo, T., Brunini, A., 2002. Are there many inactive Jupiter-family comets among the near-Earth asteroid population? Icarus 159, 358–368.

Ferraz-Mello, S., Michtchenko, T.A., Nesvorný, D., Roig, F., Simula, A., 1998. The depletion of the Hecuba gap vs. the long-lasting Hilda group. Planet. Space Sci. 46 (11/12), 1425–1432.

Fujiwara, A., Cerroni, P., Davis, D.R., Ryan, E., Di Martino, M., Holsapple, K.A., Housen, K.R., 1989. Experiments and scaling laws for catastrophic collisions. In: Binzel, R., Gehrels, T., Matthews, M.S. (Eds.), Asteroids II. Univ. of Arizona Press, Tucson, pp. 240–265.

Gault, D.E., Shoemaker, E.M., Moore, H.J., 1963. Spray ejected from the lunar surface by meteoroid impact. NASA TN D-1767.

Gil Hutton, R., Brunini, A., 2000. Collisional evolution of the outer asteroid belt. Icarus 145, 382–390.

Gladman, B.J., Migliorini, F., Morbidelli, A., Zappala, V., Michel, P., Cellino, A., Froeschle, C., Levison, H., Bailey, M., Duncan, M., 1997. Dynamical lifetimes of objects injected into asteroid belt resonances. Science 277, 197–201.

Greenberg, R., Wacker, J.F., Hartmann, W.K., Chapman, C.R., 1978. Planetesimals to planets: numerical simulation of collisional evolution. Icarus 35, 1–26.

Harris, A.W., Kaula, W.M., 1975. A co-accretional model of satellite formation. Icarus 24, 516–524.

Jewitt, D.C., Trujillo, C.A., Luu, J.X., 2000. Population and size distribution of small jovian Troyan asteroids. Astron. J. 120, 1140–1147.

Levison, H., Duncan, M., 1997. From the Kuiper Belt to Jupiter-family comets: the spatial distribution of ecliptic comets. Icarus 127, 13–32.

Levison, H., Duncan, M., Zahnle, K., Holman, M., Dones, L., 2000. Planetary impact rates from ecliptic comets. Note. Icarus 143, 415–420.

Mc Kinnon, W.B., Chapman, C.R., Housen, K.R., 1991. Cratering of the uranian satellites. In: Bergstrahl, J.T., Miner, E.D., Matthews, M.S. (Eds.), Uranus. Univ. of Arizona Press, Tucson, pp. 629–692.

Moore, J.M., 25 colleagues, 2001. Impact features on Europa: results of the Galileo Europa mission. Icarus 151, 93–111.

Nesvorný, D., Ferraz-Mello, S., 1997. On the asteroidal population of the first-order jovian resonances. Icarus 130, 247–258.

Roig, F., Nesvorný, D., Ferraz-Mello, S., 2002. Asteroids in the 2 : 1 resonance with Jupiter: dynamics and size distribution. Mon. Not. R. Astron. Soc. 335, 417–431.

Safronov, V.S., 1969. Evolution of the Protoplanetary Cloud and Formation of the Earth and Planets. Nauka, Moscow. English transl.: NASA TTF-677, 1972.

Schmidt, R.M., Housen, K.R., 1987. Some recent advances in the scaling of impact and explosion cratering. Int. J. Impact Eng. 5, 543–560.

Zahnle, K., Levison, H., Dones, L., 1998. Cratering rates on the Galilean satellites. Icarus 136, 202–222.

Zapalá, V., Farinella, P., Knezevic, Z., Paolicchi, P., 1984. Collisional origin of asteroid families: mass and velocity distribution. Icarus 59, 261–285.